Tracking Tidal Volume From Holter and Wearable Armband Electrocardiogram Monitoring

Jesús Lázaro, Natasa Reljin, Raquel Bailón, Eduardo Gil, Yeonsik Noh, Pablo Laguna, *Fellow, IEEE*, and Ki H. Chon, *Fellow, IEEE*

***Abstract*—A novel method for tracking the tidal volume (TV) from electrocardiogram (ECG) is presented. The method is based on the amplitude of ECG-derived respiration (EDR) signals. Three different morphology-based EDR signals and three different amplitude estimation methods have been studied, leading to a total of 9 amplitude-EDR (AEDR) signals per ECG channel. The potential of these AEDR signals to track the changes in TV was analyzed. These methods do not need a calibration process. In addition, a personalized-calibration approach for TV estimation is proposed, based on a linear model that uses all AEDR signals from a device. All methods have been validated with two different ECG devices: a commercial Holter monitor, and a custom-made wearable armband. The lowest errors for the personalized-calibration methods, compared to a reference TV, were −3.48% [−17.41% / 12.93%] (median [first quartile / third quartile]) for the Holter monitor, and 0.28% [−10.90% / 17.15%] for the armband. On the other hand, medians of correlations to the reference TV were higher than 0.8 for uncalibrated methods, while they were higher than 0.9 for personal-calibrated methods. These results suggest that TV changes can be tracked from ECG using either a conventional (Holter) setup, or our custom-made wearable armband. These results also suggest that the methods are not as reliable in applications that induce small changes in TV, but they can be potentially useful for detecting large changes in TV, such as sleep apnea/hypopnea and/or exacerbations of a chronic respiratory disease.**

***Index Terms*—Wearable devices, electrocardiogram (ECG), ECG-derived respiration, ECG-derived tidal volume.**

Manuscript received 2 November 2023; revised 7 February 2024 and 12 March 2024; accepted 25 March 2024. Date of publication 1 April 2024; date of current version 6 June 2024. This work was supported in part by the European Union's Framework Programme for Research and Innovation Horizon 2020 (2014-2020), under the Marie Skłodowska-Curie Grant 745755, in part by Grant PID2021-126734OB-C21 and Grant PID-2022-138585OA-C32 funded by MCIN/ AEI /10.13039/501100011033/ and by "ERDF A way of making Europe"; Grant PDC2021-120775-I00 and TED2021-131106B-I00 funded by MCIN/ AEI /10.13039/501100011033/ and by the "European Union NextGenerationEU/PRTR", in part by Gobierno de Aragon, Reference Group BSICoS T39-23R, in part by the University of Zaragoza under Project UZ2022-IAR-06, in part by Fundacion Universitaria Antonio Gargallo under Grant 2022/B004 and Grant 2023/B002, in part by N I H R43 HL under Grant 135961, and in part by NSFSBIR Phase I under Grant 1746589. *(Corresponding author: Jesús Lázaro.)*

This work involved human subjects or animals in its research. Approval of all ethical and experimental procedures and protocols was granted by Institutional Review Board at the University of Connecticut (Protocol H16-107), and performed in line with the Declaration of Helsinki.

Jesús Lázaro, Raquel Bailón, Eduardo Gil, and Pablo Laguna are with Biomedical Signal Interpretation and Computational Simulation Group, Aragón Institute of Engineering Research (I3A), IIS Aragón, University of Zaragoza, 50018 Zaragoza, Spain, and also with CIBER de Bioingeniería, Biomateriales y Nanomedicina (CIBER-BBN), 28029, Spain (e-mail: jlazarop@unizar.es).

Natasa Reljin was with the Biomedical Engineering Department, University of Connecticut, Storrs, CT 06269 USA.

Yeonsik Noh is with College of Nursing, University of Massachussetts, Amherst, MA 01003 USA, and also with the Department of Electrical and Computer Engineering, University of Massachussetts, Amherst, MA 01003 USA.

Ki H. Chon is with Biomedical Engineering Department, University of Connecticut, Storrs, CT 06269 USA.

Digital Object Identifier 10.1109/JBHI.2024.3383232

I. Introduction

TIDAL volume (TV) is the volume of air inhaled or exhaled during a respiratory cycle. Together with respiratory rate, TV regulates the minute ventilation and thus, it remains one of the most important descriptors of respiratory activity from a clinical view point. The ideal respiratory monitor would provide continuous information about TV, respiratory rate and the degree of gas exchange taking place in a non-obtrusive fashion [1]. In addition, assessment of TV from electrocardiogram (ECG) would be interesting in many clinical applications, such as sleep studies, mechanical ventilation and monitoring respiratory diseases [2]. In fact, respiratory rate has been used as a marker in several applications that may benefit from the detection of changes in minute ventilation and thus, TV may also be an interesting indicator in such applications. These applications include stress assessment [3], epileptic seizure detection [4], chronic obstructive pulmonary disease classification [5], and dynamic lung compliance assessment [6].

Techniques for monitoring respiration and, in particular, TV, are usually based on cumbersome devices which are highly inconvenient in some applications, such as sleep studies or daily life monitoring. The gold standard technique for respiratory volume monitoring is spirometry, which requires the subject to breathe through a mouthpiece connected to a pipe. This pipe measures air flow (e.g., with turbines or pilot tubes), which is later used for calculating air volume by integration in time [7]. Later, TV can be obtained from maximum and minimum air volume of the respiratory cycle. An alternative technique

that does not require to breathe through a pipe is the whole chest-abdomen plethysmography. This technique consists of measuring the volume changes of chest and abdomen by using two separate plethysmography bands, followed by estimating the tidal volume from changes in impedance values. However, this technique requires calibration for the specific location of the bands employed, and its accuracy is highly dependent on immobility of the bands [8].

Because of these limitations of the standard respiration monitoring techniques, some alternatives for assessing respiratory information have been proposed in the literature. Most of these alternatives are based on ECG signals, leading to the so-called ECG-derived respiration (EDR) techniques [9], [10]. However, most of these techniques are usually evaluated for estimation of respiratory rate, while the number of studies aimed to derive TV from the ECG is rather scant albeit smartphone camera was used to estimate TV and respiratory rates [11], [12]. Variations in QRS area were studied in [13]. Peak-to-peak change in the direction of vectorcardiogram loops [14], and a root-mean-square-based measurement of QRS amplitude have been used to estimate TV from mechanically-ventilated Yorkshire swine in [15]. In [16], TV was estimated from ECG signals based on both heart rate and EDR features during an exercise stress test. However, the features based on mean heart rate were the most important in those methods, and so the interpretation of the results is considerably limited because the method mainly tracks changes in mean heart rate and not TV (given the high correlation of mean heart rate and TV during an exercise stress test).

In [17], a pilot study on tracking changes in TV using ECG signals acquired by a wearable armband was presented. This wearable armband is a self-developed device that records, among other signals, three ECG channels. This device has been previously evaluated as heart rate monitor during daily life [18], atrial fibrillation detection [19], and as respiratory rate monitor [20]. In [17], three EDR techniques were applied, and a linear correlation between TV and the peak-to-peak amplitude of the obtained EDR signals was observed. This observation suggest that EDR techniques are potentially applicable to track changes in TV by means of their amplitude, although only five recordings were analyzed.

In this paper, the study from [17] has been evolved. A method for tracking TV changes from ECG based on the amplitude of EDR signals (AEDR) is proposed. Three different strategies for estimating the amplitude of the EDR signals were explored: peak-to-peak amplitude, root mean square (RMS), and the magnitude of the analytic signal. In addition, a personalized model for TV estimation was developed. Methods were evaluated with 28 recordings that include ECG signals by two different devices: a commercial Holter Monitor, and the self-developed ECG wearable armband [18], allowing a comparison of conventional and wearable setups.

II. Materials and Methods

A. Data Acquisition and Preprocessing

ECG and spirometry signals were simultaneously recorded from 14 healthy volunteers (ages ranging from 19 to 52 years, gender: 11 males and 3 females) during an experiment which included TV changes. The experiments were performed twice for each subject, resulting in 28 recordings. Time between experiments was 21.5 ± 3.0 minutes (mean $\pm$ standard deviation), and devices were not removed between two experiments. The experimental protocol was approved by the Institutional Review Board at the University of Connecticut (Protocol H16-107). Subjects were requested to breathe through a spirometer while looking at its output signal on a computer screen in order to have visual feedback. The subjects were asked to breathe with a small TV at the beginning, and to increase TV in small steps each 3 respiratory cycles, i.e., subjects were requested to maintain a respiratory depth for 3 cycles and then, slightly increase this depth. Subjects were requested to keep on increasing their TV 3 cycles by 3 cycles as long as they felt comfortable and then, to decrease their TV in a similar way (slightly decrease depth 3 cycles by 3 cycles). An example of breathing volume signal $x_{\mathrm{R}}(n)$ obtained during the above described breathing procedures can be observed in the panel (a) of Fig. 1.

Spirometer signals were obtained by the FE141 Spirometer with a MLT1000L respiratory flow head (AD Instruments, Dunedin, New Zealand) and digitized by a Powerlab analog-to-digital converter. The FE141 Spirometer is based on air flow measured by a precision differential pressure amplifier. ECG signals were recorded by 2 different devices. One of these devices is a commercial Holter monitor: Rozinn RZ 153+ (Glendale, NY, USA). This Holter monitor records three ECG channels with a sampling rate of 180 Hz. The other device is the wearable armband developed at University of Connecticut, which records three ECG channels with the sampling rate of 1000 Hz. The armband-ECG signals were preprocessed as in [18], i.e., a resampling to 250 Hz, and a band-pass filter with cutoff frequencies of 3 and 25 Hz. Respiratory rate is usually below 3 Hz (180 breaths per minute), thus, the highpass cut-off frequency of 3 Hz is practically removing the respiration modulation of ECG baseline. However, the EDR techniques used in this manuscript are based on morphological features extracted from the abrupt zones of the QRS complex (R-S amplitude and QRS slopes) thus, in the higher frequencies (similarly to an amplitude modulation). This aggressive filtering is part of the preprocessing motivated by the noise observed in the armband ECG signals during daily life [18].

A fourth ECG channel was generated for each one of the two ECG (Holter and armband) devices, by using the first component from the spatial principal component analysis (PCA) [21].

B. Electrocardiogram-Derived Respiration

Three EDR techniques that exploit the respiration-related QRS morphology changes were applied to each one of the four available ECG channels ($x_1(n)$, $x_2(n)$, $x_3(n)$, and $x_{\mathrm{PCA}}(n)$). Therefore, 12 EDR signals per experiment were obtained. The three EDR techniques used are: QRS slope range (SR) [22], R-wave angle (RWA) [23], and R-S amplitude (RS) [13], which are described below.

SR: The QRS slopes series, $d_{\mathrm{SR}}(n)$, presents oscillations that are synchronous with respiration, and they have been reported

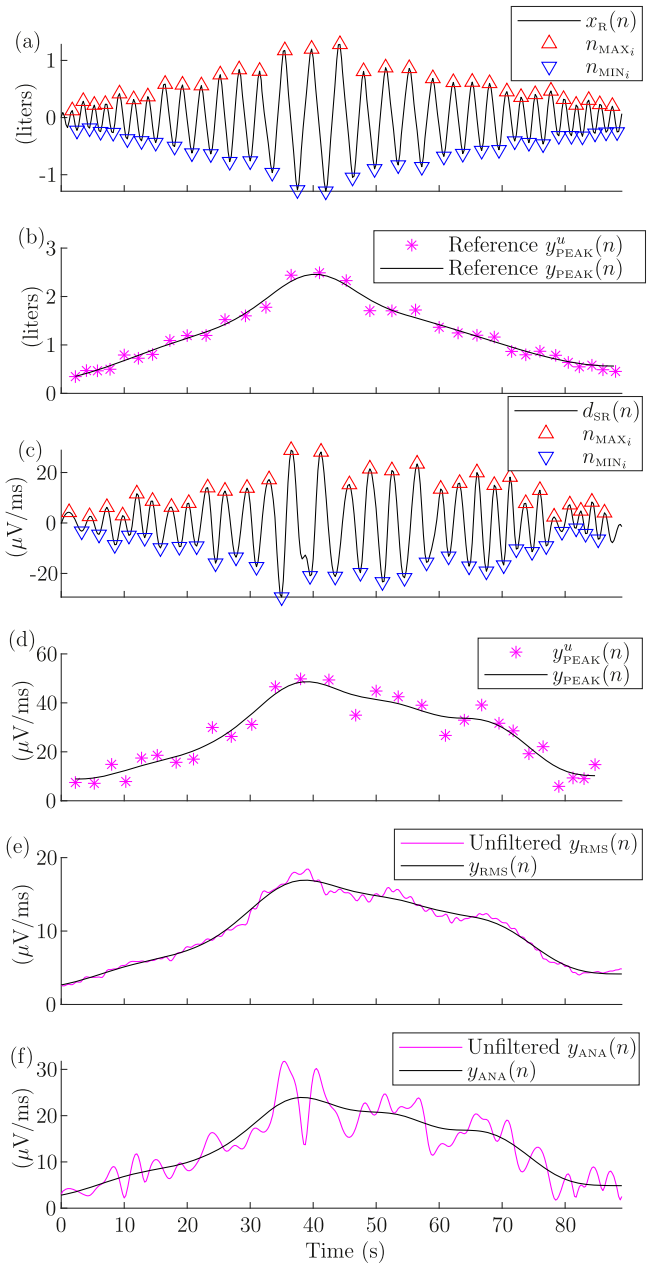

Fig. 1. (a) Example of registered respiration during the experiment involving dynamic changes in TV. Panel (b) shows the reference TV, obtained by the peak-to-peak amplitude-EDR (AEDR) estimation algorithm applied to the volume signal obtained from the spirometer shown in (a). Panel (c) shows slope-range-based EDR signal obtained from the PCA channel. Below, its estimated AEDR obtained by the three estimation algorithms are shown: peak-to-peak (d), RMS (e), and analytic (f).

to be a robust basis for respiratory rate estimation from the ECG in highly noisy and non-stationary environments [23]. These slopes are defined as the most abrupt upslope and the most abrupt downslope of the QRS complex. The SR is the difference between the two slopes, so it remains a simple method to combine the information of both slopes [22]. These features, together with RWA, obtained the best results when they were evaluated in different datasets as estimators of respiratory information of different kind, including respiration morphology [10].

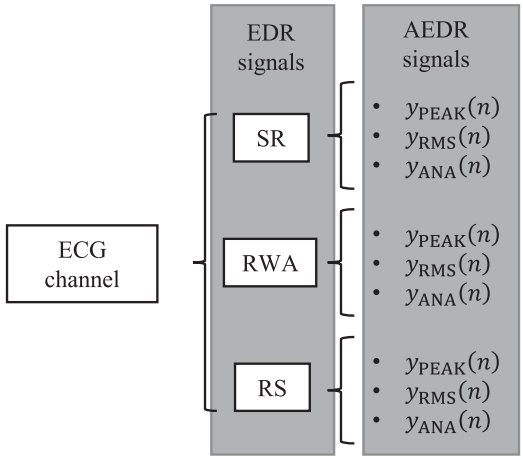

Fig. 2. Scheme of the 9 different AEDR signals obtained per ECG channel.

RWA: Similarly to the QRS slopes, the RWA series, $d_{RWA}(n)$, has also been reported as a robust respiratory rate estimator in highly noisy environments. Furthermore, RWA was reported to exhibit partially complementary information to that obtained by the QRS slopes. It is computed as the smallest angle formed by two straight lines whose slopes are the QRS slopes used for computing the SR [23].

RS amplitude: R-S amplitude series, $d_{RS}(n)$, is computed as the amplitude of the R peak with reference to the S peak. It remains one of the simplest methods to obtain respiratory rate from the ECG. This is the reason why this method is considered in this study, as implementation simplicity is a very valuable feature in the context of wearable devices.

C. Tidal Volume Changes Tracking

The hypothesis of this work is that AEDR series, $y(n)$, is related to the TV. Thus, various estimated AEDR signals obtained from different EDR signals and their potential to track TV changes were studied. First, EDR signals ($d(n)$) were interpolated to 4 Hz by cubic spline interpolation, and then they were band-pass filtered with cut-off frequencies of 0.075 Hz and 1 Hz as in [20], considering this frequency band as the respiration band. Then, three different techniques were studied for AEDR estimation: peak-to-peak amplitude, root mean square (RMS) value, and magnitude of the analytic signal. In this way, 9 AEDR (3 amplitude estimation methods times 3 EDR signals) signals were obtained for each ECG channel as shown in Fig. 2.

These three techniques for oscillations-amplitude estimation are well known envelope estimators in communications applications. The peak-to-peak amplitude method was chosen for its direct relation with the definition of TV (the volume of air displaced in a respiratory cycle), which can be seen as peak-to-peak amplitude of the air volume signal. However, this method is highly vulnerable to noise, and noise is certainly expected in EDR signals. On the other hand, RMS value and the magnitude of the analytic signal are less vulnerable to noise and do not require peak detection.

Peak-to-peak amplitude: This amplitude-estimation method consists of detecting the local maxima of the EDR signal that are separated at least by 1 s. This minimum separation was chosen considering the maximum respiratory rate of 1 Hz, which corresponds to the high cutoff frequency of the above-mentioned bandpass filter applied to the EDR signals. If more than one local maximum are detected in less than 1 s, then only the maximum with the highest amplitude is taken into account. Similarly, the local minima of the EDR signal that are separated at least by 1 s. were detected. Then, a sample of AEDR was estimated for each cycle by the amplitude of the detected maximum minus the amplitude of the detected minimum. This AEDR sample is associated with the middle time instant between maximum and minimum:

$$y^{u}_{\mathrm{PEAK}}(k) = \sum_{i} \left(d(n_{\mathrm{MAX_i}}) - d(n_{\mathrm{MIN_i}})\right) \delta\left(k - \frac{n_{\mathrm{MAX_i}} + n_{\mathrm{MIN_i}}}{2}\right), \quad (1)$$

where $\delta(\cdot)$ is the Kronecker delta function, $n_{\mathrm{MAX_i}}$ and $n_{\mathrm{MIN_i}}$ are the locations of the maximum and the minimum of the *i*th cycle in *d(n)*, respectively. Note that signal $y^{u}_{\mathrm{PEAK}}(k)$ is unevenly sampled. Then, a 4-Hz-evenly sampled version of $y^{u}_{\mathrm{PEAK}}(k)$ was obtained by cubic splines interpolation. Subsequently, a low-pass filter with a cut-off frequency of 0.05 Hz was applied to attenuate the high frequency noise of the AEDR estimation. Note that this cut-off frequency would allow us to track periodical changes of TV with a full period cycle of 20 s. This is a much shorter period than that forced by the studied protocol (around 100 s, see Fig. 1), which implies, at the same time, a greater TV changes compared to spontaneously breathing. The resulting peak-to-peak AEDR signal is denoted as $y_{\mathrm{PEAK}}(n)$ in this paper.

RMS value: This amplitude-estimation method is based on the RMS value of the EDR signal in a sliding window of a fixed length. In this work, this length was set to 10 s, in order to cover at least one respiratory cycle when the respiratory rate is as low as 0.1 Hz. Similar to the peak-to-peak case, a low-pass filter with a cut-off frequency of 0.05 Hz was applied. The resulting RMS AEDR signal is denoted as $y_{\mathrm{RMS}}(n)$ in this paper.

Analytic signal: This method consists of computing the EDR envelope as the magnitude of its analytic signal. The real part of the analytic signal is the original EDR signal, and the imaginary part was obtained by applying a Hilbert transform with a fixed length finite impulse response filter. Similar to the RMS AEDR case, this fixed length was set to 10 s in this work. Similar to the peak-to-peak and the RMS cases, a low-pass filter with a cut-off frequency of 0.05 Hz was applied. The resulting analytic AEDR signal is denoted as $y_{\mathrm{ANA}}(n)$ in this paper.

D. Reference Tidal Volume

As the TV is defined as the volume of air displaced in a respiratory cycle, it is computed as the peak-to-peak amplitude of a respiratory volume signal. In this work, the reference TV was obtained by applying the peak-to-peak AEDR technique to the respiratory volume signal from a spirometer. This reference TV signal is denoted $y_{\mathrm{R}}(n)$ in this paper.

E. Personalized Tidal Volume Estimation

Amplitude of EDR signals showed a very different correlation with TV for different subjects in the pilot study [17]. A linear regression was used in order to combine these amplitudes with a greater weight for those methods that more correlated with TV, obtaining higher correlations. Although this study included only 5 subjects, and the linear regression was tested with the same data that it was trained, these results suggested that these EDR signals may have complementary TV information. In order to combine the information from the 3 different EDR signals and 4 ECG channels of each device, a subject-personalized linear regression model was trained to estimate TV, using the spirometer-measured TV ($y_{\mathrm{R}}(n)$) as the reference. This model was trained independently for each subject, and for each one of the three amplitude-estimation methods described in Section II-C (peak-to-peak, RMS value, and analytic signal). This leads to 3 different models per subject that are denoted $y^{\mathrm{P}}_{\mathrm{M}}(n)$, ($\mathrm{M} \in \{\mathrm{PEAK}, \mathrm{ANA}, \mathrm{RMS}\}$) in this paper. Each one of them includes the corresponding AEDR signals ($y_{\mathrm{PEAK}}(n)$, $y_{\mathrm{RMS}}(n)$, or $y_{\mathrm{ANA}}(n)$) from the 12 EDR signals of the analyzed device (SR, RWA, and RS from ECG channels 1, 2, 3, and PCA), i.e., 12 weights (and intercept) were estimated during the training stage. These weights were estimated by least squares, with the constrain of not assigning negative weights, while no constrain was applied on intercept. In order to avoid overfitting, $y^{\mathrm{P}}_{\mathrm{M}}(n)$ was trained using the data from the first experiment of each subject, and it was evaluated using the data from the second experiment of the corresponding subject. An example of $y^{\mathrm{P}}_{\mathrm{M}}(n)$, ($\mathrm{M} \in \{\mathrm{PEAK}, \mathrm{ANA}, \mathrm{RMS}\}$) can be observed in Fig. 1. In order to assess the influence of PCA channel in the obtained results, this experiment was also performed alternatively excluding the PCA channel.

III. Results

For each of the 28 experiments (two experiments from 14 subjects), correlations between the reference TV ($y_{\mathrm{R}}(n)$) and different AEDR signals ($y_{\mathrm{M}}(n)$, $\mathrm{M} \in \{\mathrm{PEAK}, \mathrm{ANA}, \mathrm{RMS}\}$) from different ECG channels were computed. Table I shows the intersubject medians and interquartile ranges (IQRs). In addition, the number of experiments for which a correlation was higher than 0.5 (N_{05}), higher than 0.7 (N_{07}), or higher than 0.9 (N_{09}) are also shown.

With respect to the personalized TV estimation, both the absolute ($e_{\mathrm{A}}(n)$) and the relative ($e_{\mathrm{R}}(n)$) errors were obtained:

$$e_{\mathrm{A}}(n) = y^{\mathrm{P}}_{\mathrm{M}}(n) - y_{R}(n), \mathrm{M} \in \{\mathrm{PEAK}, \mathrm{ANA}, \mathrm{RMS}\} \quad (2)$$

$$e_{\mathrm{R}}(n) = \frac{e_{\mathrm{A}}(n)}{y_{\mathrm{R}}(n)}. \quad (3)$$

The intersubject median and IQR of these errors are shown in Table II. In addition, Fig. 3 shows Bland-Altman plots of the intrasubject mean of estimated TV and intrasubject mean of reference TV, for both Holter (top row) and armband (bottom row) devices when including the PCA channel. The correlations between the reference TV and the TV estimated by the personalized linear model were obtained, in both the first (train) and

TABLE I

MEDIAN AND IQR OF THE CORRELATION BETWEEN THE REFERENCE TV ($y_{\mathrm{R}}(n)$) AND THE DIFFERENT AEDR SIGNALS ($y_{\mathrm{M}}(n)$, $\mathrm{M} \in \{\mathrm{PEAK}, \mathrm{ANA}, \mathrm{RMS}\}$) OF THE DIFFERENT STUDIED ECG CHANNELS, FROM THE 2 EXPERIMENTS OF THE 14 SUBJECTS (28 EXPERIMENTS IN TOTAL)

			ECG Channel 1			ECG Channel 2			ECG Channel 3			ECG Channel PCA		
			SR	RWA	RS	SR	RWA	RS	SR	RWA	RS	SR	RWA	RS
Holter	$y_{\mathrm{PEAK}}(n)$	Median	0.88	0.83	0.84	0.76	0.77	0.82	0.80	0.91	0.86	0.83	0.83	0.85
		IQR	0.15	0.23	0.33	0.34	0.43	0.42	0.30	0.30	0.31	0.23	0.16	0.39
		N_{05}	**26**	25	23	**23**	21	21	22	**23**	22	**26**	25	22
		N_{07}	**24**	22	19	15	17	**19**	**20**	**20**	19	22	**24**	18
		N_{09}	**11**	10	10	9	**10**	**10**	12	**15**	11	**11**	8	9
	$y_{\mathrm{RMS}}(n)$	Median	0.89	0.87	0.87	0.82	0.85	0.85	0.88	0.92	0.89	0.87	0.86	0.84
		IQR	0.14	0.19	0.29	0.26	0.38	0.27	0.31	0.21	0.34	0.28	0.18	0.29
		N_{05}	**25**	23	24	**23**	22	22	**23**	22	**23**	**26**	24	23
		N_{07}	**24**	22	20	20	16	**21**	20	**21**	19	20	**22**	20
		N_{09}	**14**	13	13	9	11	**12**	13	**16**	13	**12**	11	10
	$y_{\mathrm{ANA}}(n)$	Median	0.89	0.87	0.86	0.82	0.83	0.84	0.84	0.89	0.88	0.82	0.82	0.82
		IQR	0.18	0.23	0.24	0.24	0.30	0.27	0.33	0.20	0.37	0.23	0.20	0.28
		N_{05}	**25**	23	24	**24**	23	21	22	**24**	23	**26**	25	24
		N_{07}	**23**	21	21	20	17	**21**	20	**21**	20	**22**	21	20
		N_{09}	12	**13**	12	7	**11**	10	**13**	12	12	10	**11**	9
Armband	$y_{\mathrm{PEAK}}(n)$	Median	0.87	0.93	0.78	0.88	0.91	0.85	0.89	0.92	0.85	0.87	0.91	0.85
		IQR	0.23	0.11	0.26	0.18	0.19	0.27	0.16	0.13	0.33	0.15	0.14	0.22
		N_{05}	**26**	**26**	22	**26**	**26**	23	**24**	**24**	24	**26**	**26**	22
		N_{07}	21	**25**	17	22	**23**	19	**24**	22	18	**24**	**24**	21
		N_{09}	11	**16**	9	13	**17**	6	13	**17**	12	11	**15**	10
	$y_{\mathrm{RMS}}(n)$	Median	0.90	0.93	0.85	0.89	0.92	0.79	0.83	0.90	0.84	0.89	0.91	0.86
		IQR	0.24	0.24	0.57	0.24	0.16	0.38	0.34	0.24	0.22	0.24	0.18	0.56
		N_{05}	22	**24**	19	22	**26**	22	22	**23**	23	24	**25**	19
		N_{07}	21	**23**	17	21	**23**	17	20	**22**	21	**22**	**22**	17
		N_{09}	15	**18**	11	13	**16**	10	11	**14**	10	13	**15**	12
	$y_{\mathrm{ANA}}(n)$	Median	0.88	0.91	0.83	0.87	0.91	0.75	0.85	0.88	0.81	0.88	0.89	0.83
		IQR	0.22	0.18	0.46	0.18	0.15	0.32	0.29	0.26	0.23	0.15	0.14	0.45
		N_{05}	24	**25**	20	24	**26**	23	23	**24**	22	**25**	**25**	20
		N_{07}	22	**23**	17	21	**24**	18	20	20	**21**	**22**	**22**	19
		N_{09}	12	**17**	8	10	**16**	6	10	**13**	9	9	**14**	8

N_{05}, N_{07}, and N_{09} represent the number of experiments (out of the 28 possible) for which the correlation is higher than 0.5, 0.7, or 0.9, respectively. The highest N_{05}, N_{07}, and N_{09} for each ecg channel and amplitude-estimation method is shown in bold.

TABLE II

MEDIAN, FIRST, AND THIRD QUARTILE OF BOTH ABSOLUTE (e_{A}) AND RELATIVE (e_{R}) ERRORS OF THE TV ESTIMATION BY THE PERSONALIZED LINEAR MODEL ($y^{\mathrm{P}}_{\mathrm{M}}$, $\mathrm{M} \in \{\mathrm{PEAK}, \mathrm{ANA}, \mathrm{RMS}\}$) WITH RESPECT TO THE REFERENCE TV OBTAINED FROM THE SPIROMETER ($y_{\mathrm{R}}(n)$), IN THE VALIDATION SET (SECOND EXPERIMENT OF EACH SUBJECT)

		Including PCA channel				Excluding PCA channel			
		Holter		Armband		Holter		Armband	
		Median	Q1 / Q3	Median	Q1 / Q3	Median	Q1 / Q3	Median	Q1 / Q3
$y^{\mathrm{P}}_{\mathrm{PEAK}}(n)$	e_{A} (ml)	3	-113 / 338	73	11 / 207	15	-160 / 337	64	6 / 108
	e_{R} (%)	0.24	-14.87 / 34.74	8.12	1.76 / 20.61	1.57	-16.75 / 34.74	6.29	0.55 / 15.38
$y^{\mathrm{P}}_{\mathrm{RMS}}(n)$	e_{A} (ml)	-52	-311 / 164	5	-91 / 166	-69	-329 / 164	-8	-135 / 159
	e_{R} (%)	-4.29	-27.18 / 15.71	0.65	-11.43 / 12.18	-5.47	-27.56 / 15.71	-0.74	-22.70 / 11.17
$y^{\mathrm{P}}_{\mathrm{ANA}}(n)$	e_{A} (ml)	-19	-248 / 123	8	-94 / 231	-19	-234 / 123	3	-87 / 226
	e_{R} (%)	-3.45	-22.42 / 12.93	0.88	-11.87 / 17.15	-3.48	-17.41 / 12.93	0.28	-10.90 / 17.15

the second (test) experiments. Intersubject medians and IQRs of these correlations are shown in Table III, where the number of experiments for which a correlation higher than 0.5 (N_{05}), higher than 0.7 (N_{07}), and higher than 0.9 (N_{09}) are also shown. It is noteworthy that in this case, the total number of experiments in each one of the columns is 14 (one per subject), while it is 28 (two per subject) in the case of Table I.

IV. DISCUSSION

A novel method for tracking TV from ECG has been presented. Recognizing that the respiratory-related modulation of the ECG morphology is stronger when the TV is higher, the method for estimation of TV is based on AEDR signals. The methods have been validated with two different ECG devices:

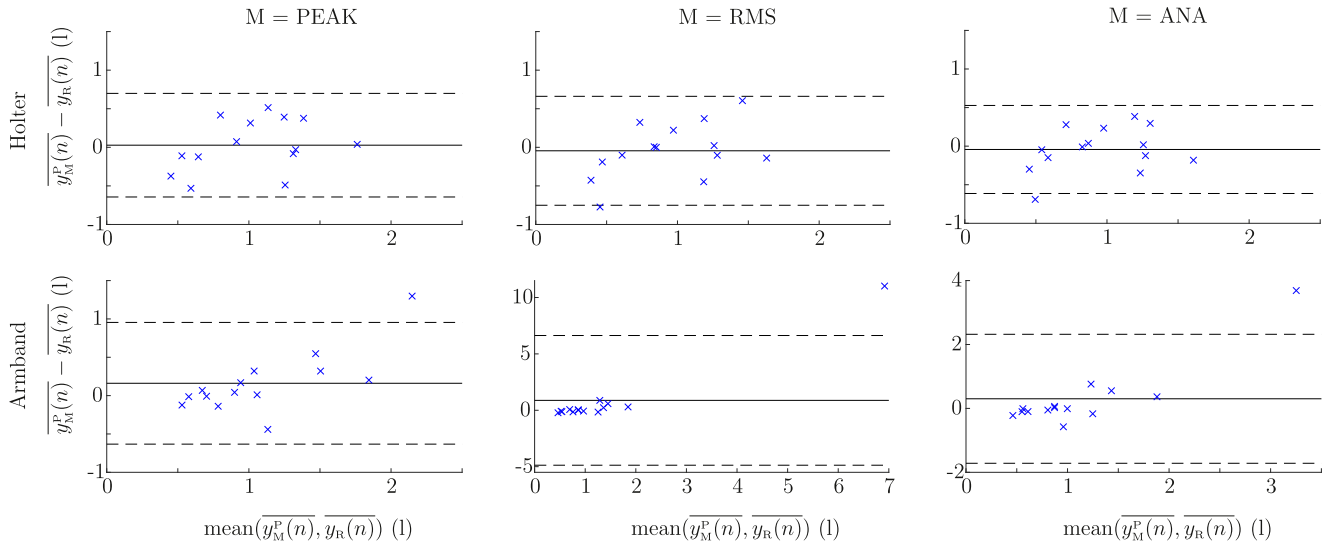

Fig. 3. Bland-Altman plots of the intrasubject mean of estimated TV ($\overline{y_{\mathrm{M}}^{\mathrm{P}}(n)}, \mathrm{M} \in \{\mathrm{PEAK},\ \mathrm{RMS},\ \mathrm{ANA}\}$) and intrasubject mean of reference TV ($\overline{y_{\mathrm{R}}(n)}$), for both devices Holter (top row) and armband (bottom row) when including the PCA channel. Note that different axis limits are used for the armband in cases of RMS and ANA in order to show an outlier.

TABLE III
INTERSUBJECT MEDIAN AND IQR OF THE CORRELATION BETWEEN THE REFERENCE TV ($y_{\mathrm{R}}(n)$) AND THE TV ESTIMATED BY THE PERSONALIZED LINEAR REGRESSION MODEL ($y_{\mathrm{M}}^{\mathrm{P}},\ \mathrm{M} \in \{\mathrm{PEAK}, \mathrm{ANA}, \mathrm{RMS}\}$)

		Including PCA channel				Excluding PCA channel			
		Holter		Armband		Holter		Armband	
		Train	Test	Train	Test	Train	Test	Train	Test
$y_{\mathrm{PEAK}}^{\mathrm{P}}(n)$	Median	0.97	0.90	0.95	0.89	0.98	0.85	0.95	0.89
	IQR	0.04	0.33	0.06	0.19	0.03	0.45	0.07	0.17
	N_{05}	13	9	14	12	13	10	14	12
	N_{07}	13	9	14	11	13	8	13	12
	N_{09}	12	6	12	6	12	6	12	7
$y_{\mathrm{RMS}}^{\mathrm{P}}(n)$	Median	0.99	0.96	0.97	0.91	0.99	0.96	0.97	0.91
	IQR	0.06	0.18	0.03	0.35	0.06	0.18	0.03	0.35
	N_{05}	13	12	14	11	13	12	14	11
	N_{07}	13	12	14	10	13	12	14	10
	N_{09}	12	10	12	7	12	10	12	7
$y_{\mathrm{ANA}}^{\mathrm{P}}(n)$	Median	0.98	0.96	0.97	0.92	0.98	0.95	0.97	0.93
	IQR	0.06	0.12	0.05	0.20	0.06	0.12	0.05	0.21
	N_{05}	13	12	14	12	13	12	14	12
	N_{07}	13	12	14	11	13	12	14	11
	N_{09}	13	10	13	8	13	10	13	8

N_{05}, N_{07}, and N_{09} represent the number of experiments (of the 14 possible) for which a correlation higher than 0.5, 0.7, or 0.9, respectively.

a commercial Holter monitor, and a custom-made wearable armband. Both devices provide three ECG channels, and one additional channel per device has been synthesized by the first PCA component of their original three channels.

Three different morphology-based EDR signals have been studied: SR, RWA, and RS. SR and RWA were chosen because they have shown to be robust features for respiratory rate estimation from the ECG in highly noisy and non-stationary environments [23], while RS was chosen because of its computational simplicity.

In order to estimate the amplitudes of EDR signals, three AEDR methods have been studied: peak-to-peak envelope, RMS envelope, and the absolute value of the analytic signal. The reference TV was obtained from a spirometer-based volume signal by the peak-to-peak AEDR method. The reason for this is that the clinical definition of TV is the volume of air displaced in a respiratory cycle and thus, it is estimated by calculating the peak-to-peak amplitude of a respiratory volume signal.

All AEDR signals were obtained from a dataset that includes ECG data from an experiment involving considerable TV changes that was performed twice per subject. Intersubject medians of correlations between these AEDR signals and the reference TV were strong (>0.7) in every case, for both Holter and the armband. These median correlations are higher than

that reported in [15] (0.67, median $R^2 = 0.44$) when estimating TV from individual ECG leads. However, these numbers should not be directly compared because the evaluation in this study is performed with conscious humans while the evaluation in [15] is performed with sedated mechanically-ventilated Yorkshire swine.

Results show very different correlations for different recordings in some cases, e.g., a correlation higher than 0.9 was obtained for at least 10 recordings in almost every case while at least 2 recordings obtained a correlation lower than 0.5 in every case. A possible explanation for this observation is that during those recordings with low correlations, subjects may have been breathing with a very predominant abdominal breathing pattern. The effects that cause respiration-related modulations in ECG are the movement of the electrodes with respect to the heart, and the impedance changes in the chest due to the filling/emptying of the lungs. It is reasonable to expect that those effects are greater during a thoracic breathing pattern. Unfortunately, a reference for breathing pattern is not available in this study, so this hypothesis cannot be studied with the available data.

The gender of the subjects in the data set is unbalanced, with 3 women and 11 men. Thus, it is not possible to analyze differences in performance of the methods in different genders. As a note, no differences in genders were observed when using these methods for respiratory rate estimation in [23].

Non-calibrated TV-tracking with the Holter device: Regarding the Holter, the median correlation was higher than 0.9 in the case of $y_{\text{PEAK}}(n)$ and $y_{\text{ANA}}(n)$ from the RWA EDR signal for channel 2 of the Holter device.

Among the 28 recordings, N_{05} (the number of experiments with correlation greater than 0.5) ranged from 21 up to 26. This means that at least moderate correlation (>0.5) was obtained between 75.00% and 92.86% of the recordings, depending on the case (ECG channel, EDR signal, and AEDR method). N_{07} ranged from 15 up to 24, so at least strong correlation (>0.7) was obtained between 53.57% and 85.71% of the recordings, depending on the case. N_{09} ranged from 7 up to 16, so very strong correlation (>0.9) was obtained between 25% and 57.14% of the recordings, depending on the case. Focusing on N_{05}, N_{07}, N_{09} for different AEDR signals from the PCA channel (which combines the other 3 ECG channels), RWA obtained the highest value in 6 cases, while SR obtained the highest value in 3 cases, and RS did not obtain the highest value in any case (see bold numbers in Table I).

However, the results in these metric features are very similar across different EDR signals (SR, RWA, and RS), and also across different amplitude estimation methods ($y_{\text{PEAK}}(n)$, $y_{\text{RMS}}(n)$, and $y_{\text{ANA}}(n)$). With respect to different EDR signal, this observation is expected when taking into account non-noise corrupted scenarios. SR and RWA (both of them based on QRS slopes) were proposed as robust alternatives to other morphology-based methods, such as the RS [23], and they do not represent significant advantages in a very low level of noise. Similar reasoning can be applied with respect to different methods to estimate the envelope. The three of them are well-known methods to estimate the envelope of a signal, and they should work properly in a low-noise-level scenario. Further experiments in the presence of a higher level of noise must be performed in order to assess the degradation of the performance of different AEDR signals in tracking TV.

Non-calibrated TV with the armband device: Regarding the armband, the median correlation was higher than 0.9 for $y_{\text{PEAK}}(n)$ and $y_{\text{RMS}}(n)$ from the RWA EDR signal for all the ECG channels, and also for $y_{\text{ANA}}(n)$ from the RWA EDR for channels 1 and 2.

Among the 28 recordings, N_{05} ranged from 19 up to 26. This means that at least moderate correlation (>0.5) was obtained between 67.86% and 92.86% of the recordings, depending on the case (ECG channel, EDR signal, and AEDR method). N_{07} ranged from 17 up to 24, so at least strong correlation (>0.7) was obtained between 60.71% and 85.71% of the recordings, depending on the case. N_{09} ranged from 6 up to 17, so very strong correlation (>0.9) was obtained between 21.43% and 60.71% of the recordings, depending on the case. Focusing on N_{05}, N_{07}, N_{09} for different AEDR signals from the PCA channel, observations are aligned that RWA obtained the highest value in all 9 cases, while SR obtained the highest value in 5 cases, but SR did not obtain the highest value in any case. Similar to the case of the Holter device, results are comparable across different EDR signals and different amplitude estimation methods. However, in the case of the armband device, the RWA EDR signal consistently obtained better results than RS, and better or equal results than SR. While the scenario still involves a low level of noise, the armband setup is more challenging than the Holter setup, and these results suggest that the robustness of SR and, particularly RWA, represents an advantage over RS in the case of the former device.

Calibrated and personalized TV estimation and tracking: For each subject and each amplitude estimation method, a linear regression model using AEDR signals from all ECG channels was fitted to the reference TV. This way, 12 AEDR signals (estimated amplitude from SR, RWA, and RS-derived EDR signals from ECG channels 1, 2, 3, and PCA) were used in the linear regression model. The fitting (training) was performed with the data from the first experiment of each subject and was validated (tested) with the data from the second experiment.

Obtained medians, first, and third quartiles of absolute and relative errors (see Table II) suggest that TV estimation is not as accurate as those EDR techniques estimating respiratory rate [20], [23]. Bland-Altman plots (see Fig. 3) do not show any systematic bias in the estimations of TV, but it shows an outlier in the case of the armband device using the three amplitude-estimation methods. The best amplitude-estimation method in terms of relative and absolute error was $y_{\text{ANA}}(n)$ for the Holter monitor (with a median of -19 ml and first and third quartiles of -248 and 123 ml), and $y_{\text{RMS}}(n)$ for the armband device (with a median of 5 ml and first and third quartiles of -91 and 166 ml). These results suggest that estimation is not reliable in applications that require to accurately differentiate between small changes in TV, such as exercise monitoring or fine stress level assessment. However, the proposed method may be applicable and reliable in applications that result in bigger changes in TV, such as detection of sleep apnea/hypopnea and/or exacerbations of a chronic respiratory disease. The utility of the

methods for specific applications should be assessed in future studies.

Furthermore, results showed a very high intersubject median correlation for all three amplitude estimation methods from both the Holter and the armband devices when including the PCA channel (see Table III), suggesting that the personalized calibration process leads to a better tracking of TV. The lowest median correlations for the test set were obtained for $y^{\mathrm{P}}_{\mathrm{PEAK}}(n)$ (0.90 for the Holter and 0.89 for the armband), while correlations were higher than 0.9 for $y^{\mathrm{P}}_{\mathrm{RMS}}(n)$ and $y^{\mathrm{P}}_{\mathrm{ANA}}(n)$ for both devices. Note that the validation of the personal-calibrated method is performed with 14 recordings (as the other 14 were used for training). These median correlations are slightly higher than that reported in [15] (0.88, median $R^2 = 0.77$) when estimating TV from a combination of ECG leads. Nevertheless, it should be noted that this study presents some differences with respect to [15] that makes the direct comparison of these results inconvenient. In this study, a personalized model is trained for each subject, while a leave-one-out validation is performed in [15]. Furthermore, methods are evaluated with conscious humans in this study while they are evaluated with sedated mechanically-ventilated Yorkshire swine in [15].

An EDR signal based on the direction of the vector loop in the QRS complex was used for tracking TV in [14], combining information from different ECG leads. Correlations with TV using a linear regression were reported for 7 subjects, obtaining 0.97 / 0.05 (median / IQR) in the best case. However, the models were not tested with different data. Thus, the comparison of these results reported in [14] with those results reported in this paper should be performed with those results obtained for the training set, keeping in mind that this set is composed of 14 subjects. When using the Holter device, the peak-to-peak amplitude estimation method obtained similar correlations (0.97 / 0.04), while both RMS and analytic methods obtained slightly higher correlations (0.99 / 0.06 and 0.98 /0.06, respectively). When using the armband device, the peak-to-peak amplitude-estimation method obtained slightly lower correlations (0.95 / 0.06), while both RMS and analytic methods similar correlations (0.97 / 0.03 and 0.97/0.05, respectively).

In the case of the Holter device when including the PCA channel, the lower values of N_{05}, N_{07}, and N_{09} in the test set were obtained for $y^{\mathrm{P}}_{\mathrm{PEAK}}(n)$ (9, 9, and 6, respectively), while in both cases $y^{\mathrm{P}}_{\mathrm{RMS}}(n)$ and $y^{\mathrm{P}}_{\mathrm{ANA}}(n)$ 12 recordings (85.71%) showed at least strong correlation (>0.7) and 10 recordings (71.43%) showed very strong correlation (>0.9). Thus, similar results were obtained by $y^{\mathrm{P}}_{\mathrm{RMS}}(n)$ and $y^{\mathrm{P}}_{\mathrm{ANA}}(n)$ for the Holter device, however, a slightly better performance can be observed for $y^{\mathrm{P}}_{\mathrm{ANA}}(n)$ in terms of IQR of correlations (0.12 vs. 0.18). On the other hand, $y^{\mathrm{P}}_{\mathrm{PEAK}}(n)$, $y^{\mathrm{P}}_{\mathrm{RMS}}(n)$, and $y^{\mathrm{P}}_{\mathrm{ANA}}(n)$ obtained similar values of N_{05}, N_{07}, and N_{09} in the test set in the case of the armband. However, $y^{\mathrm{P}}_{\mathrm{ANA}}(n)$ obtained the best results in these terms. These results suggest that using $y^{\mathrm{P}}_{\mathrm{ANA}}(n)$ is more convenient than using $y^{\mathrm{P}}_{\mathrm{PEAK}}(n)$ and $y^{\mathrm{P}}_{\mathrm{RMS}}(n)$ in terms of accuracy of TV tracking.

However, the intersubject median correlation was consistently higher for the Holter than for the armband device, suggesting that the estimation with the Holter device is more robust than the estimation with the armband, and the observed differences in correlation values could be higher when involving a higher level of noise. This is expected because the armband setup (dry electrodes over the upper arm) is more challenging (e.g., an arm location rather than the chest) than the Holter setup (hydrogel electrodes over the chest). Furthermore, the armband can slightly move around the upper arm from the training set recordings to the test set recordings, resulting in slightly different ECG data than those used for training the model. However, this issue is not expected with the Holter setup, since its electrodes are attached to the chest with adhesive. This may explain why the difference in performance when using the test set with respect to the train set is higher for the armband device than for the Holter (see Table III).

Alternatively, the model was calibrated without using the EDR signals from the PCA channel. Obtained results were very similar in terms of both error (see Table II) and correlation (see Table III). These results suggest that the PCA channel is not adding any complementary information to the other ECG channels and thus, that its computation could be avoided without losing accuracy on TV tracking. However, it should be noted that this study is performed in laboratory-controlled conditions. The PCA channel has been proposed in the literature for cleaning ECG signals and offered advantages when monitoring heart rate with the armband during daily life [18]. Further experiments including more noisy scenarios should be conducted to assess the advantages of including PCA channel.

V. Conclusion

A novel method for tracking tidal volume changes from ECG has been presented, exploiting the amplitude of morphology-based EDR signals. The method has been validated with ECG data from a commercial Holter device and also with data from a custom-made wearable armband device. The lowest errors with respect to the reference TV obtained for the personal-calibrated methods were −3.48% [−17.41% / 12.93%] (median [first quartile / third quartile]) for the Holter monitor, and 0.28% [−10.90% / 17.15%] for the armband. On the other hand, medians of correlations with the reference TV were higher than 0.8 for the uncalibrated methods, while they were higher than 0.9 for the personal-calibrated methods. The inclusion of PCA ECG channel did not show advantages, probably because the scenario did not involve a high level of noise.

These results suggest that TV changes can be tracked from the ECG, either using a conventional (Holter), or our custom-made wearable armband. However, it should be noted that the methods are not reliable in applications that require accurate differentiation between small changes in TV such as exercise monitoring or fine stress level assessment. For applications that induce large changes in TV, such as sleep apnea/hypopnea and/or exacerbations of a chronic respiratory disease, the proposed approach has potential utility. The breathing pattern (thoracic/abdominal) may have an effect on the accuracy of the methods. The benefit of the proposed approaches for specific applications should be assessed in future studies. The observations reported in this manuscript should be taken into account when selecting an ECG-based feature set for a classification problem related to breathing.

REFERENCES

[1] M. Folke, L. Cernerud, M. Ekström, and B. Hök, "Critical review of non-invasive respiratory monitoring in medical care," *Med. Biol. Eng. Comput.*, vol. 41, no. 4, pp. 377–383, Jul. 2003, doi: 10.1007/bf02348078.

[2] L. Brochard et al., "Tidal volume reduction for prevention of ventilator-induced lung injury in acute respiratory distress syndrome. The multicenter trail group on tidal volume reduction in ARDS," *Amer. J. Respir. Crit. Care Med.*, vol. 158, no. 6, pp. 1831–1838, Dec. 1998, doi: 10.1164/ajrccm.158.6.9801044.

[3] A. Hernando et al., "Inclusion of respiratory frequency information in heart rate variability analysis for stress assessment," *IEEE J. Biomed. Health Inform.*, vol. 20, no. 4, pp. 1016–1025, Jul. 2016, doi: 10.1109/JBHI.2016.2553578.

[4] C. Varon, K. Jansen, L. Lagae, and S. V. Huffel, "Can ECG monitoring identify seizures?," *J. Electrocardiol.*, vol. 48, no. 6, pp. 1069–1074, Dec. 2015, doi: 10.1016/j.jelectrocard.2015.08.020.

[5] H. J. Davies, P. Bachtiger, I. Williams, P. L. Molyneaux, N. S. Peters, and D. P. Mandic, "Wearable in-ear PPG: Detailed respiratory variations enable classification of COPD," *IEEE Trans. Biomed. Eng.*, vol. 69, no. 7, pp. 2390–2400, Jul. 2022, doi: 10.1109/TBME.2022.3145688.

[6] H. Yamazaki and K. Fujimoto, "A new noninvasive method for measurement of dynamic lung compliance from fluctuations on photoplethysmography in respiration," *J. Appl. Physiol.*, vol. 130, no. 1, pp. 215–225, Jan. 2021, doi: 10.1152/japplphysiol.00295.2020.

[7] A. Kouri, R. J. Dandurand, O. S. Usmani, and C.-W. Chow, "Exploring the 175-year history of spirometry and the vital lessons it can teach us today," *Eur. Respir. Rev.*, vol. 30, no. 162, Oct. 2021, Art. no. 210081, doi: 10.1183/16000617.0081-2021.

[8] P. Duffty, L. Spriet, M. H. Bryan, and A. C. Bryan, "Respiratory induction plethysmography (Respitrace): An evaluation of its use in the infant," *Amer. Rev. Respir. Dis.*, vol. 123, no. 5, pp. 542–546, May 1981, doi: 10.1164/arrd.1981.123.5.542.

[9] P. H. Charlton, T. Bonnici, L. Tarassenko, D. A. Clifton, R. Beale, and P. J. Watkinson, "An assessment of algorithms to estimate respiratory rate from the electrocardiogram and photoplethysmogram," *Physiol. Meas.*, vol. 37, no. 4, pp. 610–626, Apr. 2016, doi: 10.1088/0967-3334/37/4/610.

[10] C. Varon et al., "A comparative study of ECG-derived respiration in ambulatory monitoring using the single-lead ECG," *Sci. Rep.*, vol. 10, no. 1, Mar. 2020, Art. no. 5704, doi: 10.1038/s41598-020-62624-5.

[11] B. A. Reyes, N. Reljin, Y. Kong, Y. Nam, and K. H. Chon, "Tidal volume and instantaneous respiration rate estimation using a volumetric surrogate signal acquired via a smartphone camera," *IEEE J. Biomed. Health Inform.*, vol. 21, no. 3, pp. 764–777, May 2017, doi: 10.1109/JBHI.2016.2532876.

[12] B. A. Reyes, N. Reljin, Y. Kong, Y. Nam, S. Ha, and K. H. Chon, "Employing an incentive spirometer to calibrate tidal volumes estimated from a smartphone camera," *Sensors*, vol. 16, no. 3, Mar. 2016, Art. no. 397, doi: 10.3390/s16030397.

[13] G. B. Moody, R. G. Mark, A. Zoccola, and S. Mantero, "Derivation of respiratory signals from multi-lead ECGs," *Comput. Cardiol.*, vol. 12, pp. 113–116, 1985.

[14] M. Noshiro et al., "Indirect measurement of tidal volume by multi-lead electrocardiograms: Effect of filtering, deep breath, lead and posture," *Front. Med. Biol. Eng.*, vol. 7, no. 3, pp. 207–219, 1996.

[15] O. Sayadi, E. H. Weiss, F. M. Merchant, D. Puppala, and A. A. Armoundas, "An optimized method for estimating the tidal volume from intracardiac or body surface electrocardiographic signals: Implications for estimating minute ventilation," *Amer. J. Physiol. Heart Circulatory Physiol.*, vol. 307, no. 3, pp. H426–H436, Aug. 2014, doi: 10.1152/ajpheart.00038.2014.

[16] J. Milagro et al., "Electrocardiogram-derived tidal volume during treadmill stress test," *IEEE Trans. Biomed. Eng.*, vol. 67, no. 1, pp. 193–202, Jan. 2020, doi: 10.1109/TBME.2019.2911351.

[17] J. Lázaro et al., "Electrocardiogram derived respiration for tracking changes in tidal volume from a wearable armband," in *Proc. IEEE 42nd Annu. Int. Conf. Eng. Med. Biol. Soc.*, 2020, pp. 596–599, doi: 10.1109/EMBC44109.2020.9175486.

[18] J. Lázaro, N. Reljin, M. B. Hossain, Y. Noh, P. Laguna, and K. H. Chon, "Wearable armband device for daily life electrocardiogram monitoring," *IEEE Trans. Biomed. Eng.*, vol. 67, no. 12, pp. 3464–3473, Dec. 2020, doi: 10.1109/TBME.2020.2987759.

[19] S. K. Bashar et al., "Feasibility of atrial fibrillation detection from a novel wearable armband device," *Cardiovasc. Digit. Health J.*, vol. 2, no. 3, pp. 179–191, Jun. 2021, doi: 10.1016/j.cvdhj.2021.05.004.

[20] J. Lazaro et al., "Electrocardiogram derived respiratory rate using a wearable armband," *IEEE Trans. Biomed. Eng.*, vol. 68, no. 3, pp. 1056–1065, Mar. 2021, doi: 10.1109/TBME.2020.3004730.

[21] F. Castells, P. Laguna, L. Sörnmo, A. Bollmann, and J. M. Roig, "Principal component analysis in ECG signal processing," *EURASIP J. Adv. Signal Process.*, vol. 2007, no. 1, Dec. 2007, Art. no. 074580, doi: 10.1155/2007/74580.

[22] S. Kontaxis et al., "ECG-derived respiratory rate in atrial fibrillation," *IEEE Trans. Biomed. Eng.*, vol. 67, no. 3, pp. 905–914, Mar. 2020, doi: 10.1109/TBME.2019.2923587.

[23] J. Lázaro et al., "Electrocardiogram derived respiratory rate from QRS slopes and R-wave angle," *Ann. Biomed. Eng.*, vol. 42, no. 10, pp. 2072–2083, Oct. 2014, doi: 10.1007/s10439-014-1073-x.